Journal of Nuclear Medicine, published on January 13, 2022 as doi:10.2967/jnumed.121.263168

In vivo evaluation of six analogs of ^{11}C-ER176 as candidate ^{18}F-labeled radioligands for translocator protein 18 kDa (TSPO)

Jae-Hoon Lee[1,2], Fabrice G. Siméon[1], Jeih-San Liow[1], Cheryl L. Morse[1], Robert L. Gladding[1], Jose A. Montero Santamaria[1], Ioline D. Henter[1], Sami S. Zoghbi[1], Victor W. Pike[1], and Robert B. Innis[1]

[1]Molecular Imaging Branch, National Institute of Mental Health, National Institutes of Health, Bethesda, MD, USA; [2]Department of Nuclear Medicine, Yonsei University College of Medicine, Seoul, South Korea

Financial support: This study was funded by the Intramural Research Program of the National Institute of Mental Health, National Institutes of Health (ZIAMH002793 and ZIAMH002795).

Short running title: *In vivo* evaluation of ^{11}C-ER176 analogs

Word count: 4991

First author/Corresponding author:
Jae-Hoon Lee, MD, PhD
Molecular Imaging Branch, NIMH-NIH
10 Center Drive, Bethesda, MD 20892
Tel: 301-594-1089
Fax: 301-480-3610
Email: jae-hoon.lee@nih.gov
ORCID ID: 0000-0002-9898-9886

ABSTRACT

Due to its excellent ratio of specific to nondisplaceable uptake, the radioligand ^{11}C-ER176 can successfully image 18kDa translocator protein (TSPO), a biomarker of inflammation, in human brain and accurately quantify target density in homozygous low-affinity binders. Our laboratory sought to develop an ^{18}F-labeled TSPO positron emission tomography (PET) radioligand based on ER176 with the potential for broader distribution. This study used generic carbon-11 labeling and *in vivo* performance in monkey brain to select the most promising among six fluorine-containing analogs of ER176 for subsequent labeling with longer-lived fluorine-18.

Methods: Six fluorine-containing analogs of ER176—three fluoro and three trifluoromethyl isomers—were synthesized and labeled by ^{11}C-methylation at the secondary amide group of the respective *N*-desmethyl precursor. PET imaging was performed in monkey brain at baseline and after blockade by PK11195. Uptake was quantified using radiometabolite-corrected arterial input function. The six candidate radioligands were ranked for performance based on two *in vivo* criteria: 1) ratio of specific to nondisplaceable uptake (BP_{ND}), and 2) time stability of total distribution volume (V_T), an indirect measure of lack of radiometabolite accumulation in the brain.

Results: Total TSPO binding was quantified as V_T corrected for plasma free fraction (V_T/f_P) using Logan graphical analysis for all six radioligands. V_T/f_P at baseline was generally high (222±178 mL·cm^{-3}) and decreased by 70–90% after pre-blocking with PK11195. BP_{ND} calculated using the Lassen plot was 9.6±3.8; the *o*-fluoro radioligand exhibited the highest BP_{ND} of 12.1, followed by the *m*-trifluoromethyl (11.7) and *m*-fluoro (8.1) radioligands. For all six radioligands, V_T values reached 90% of the terminal 120-minute values by 70 minutes and

remained relatively stable thereafter with excellent identifiability (standard errors < 5%), suggesting that no significant radiometabolites accumulated in the brain.

Conclusion: All six radioligands had good BP_{ND} and good time stability of V_T. Among them, the *o*-fluoro, *m*-trifluoromethyl, and *m*-fluoro compounds were the three best candidates for development as radioligands with a fluorine-18 label.

Keywords: translocator protein, neuroinflammation, positron emission tomography, specific-to-nondisplaceable uptake, radiometabolites

INTRODUCTION

The mitochondrial protein 18-kDa translocator protein (TSPO) is highly expressed in phagocytic inflammatory cells, including activated microglia and reactive astrocytes in the brain and macrophages in the periphery (*1,2*). Although numerous positron emission tomography (PET) radioligands have been developed to image TSPO, several limitations have restricted their clinical utility for quantifying inflammation in the brain. Of these radioligands, the first-generation TSPO radioligand ^{11}C-*(R)*-PK11195 has been the most extensively studied. ^{11}C-*(R)*-PK11195 has high affinity for TSPO; however, its utility is limited by low ratio of specific-to-nondisplaceable uptake (i.e., nondisplaceable binding potential, BP_{ND}) in the brain as well as the relatively short half-life of ^{11}C (20 minutes) (*3,4*). Second-generation radioligands, such as ^{11}C-PBR28, offer a higher *in vivo* TSPO-specific signal but suffer from sensitivity to the single nucleotide polymorphism *rs6971* (*5,6*), such that low-affinity binders (LABs) have too little TSPO binding to be accurately measured. This sensitivity to the single nucleotide polymorphism both complicates the interpretation of results and requires genotyping in order to exclude LABs before imaging. Consequently, new and more effective radioligands are needed to image TSPO.

Third-generation TSPO radioligands were designed to have adequately high BP_{ND} across all *rs6971* genotypes for reliable quantification and to lack radiometabolite accumulation in the brain that interferes with the low specific signal in LABs. In this context, ^{11}C-ER176 is arguably the most promising third-generation TSPO radioligand for clinical research (*2,7*). More specifically, it displays high specific binding (>80%), adequately high BP_{ND} in LABs, and good time stability of total distribution volume (V_T) across all genotypes (*8,9*). Whole-brain BP_{ND} of ^{11}C-ER176 for LABs was 1.4±0.8, which is about the same as that for high-affinity binders with ^{11}C-PBR28 (~1.2). For all three genotypes, the V_T values of ^{11}C-ER176 stabilized within 10% of

their final values of 120 minutes by 60–90 minutes, suggesting that no significant amount of radiometabolites accumulated in the brain (*8*).

In contrast to carbon-11, fluorine-18 has several benefits for clinical PET imaging. Its relatively longer half-life (110 versus 20 minutes) allows imaging for a longer period of time and for broader distribution of the radioligand from a central radiopharmacy, giving ^{18}F-labeled radioligands greater flexibility for widespread use. However, ER176 does not contain a fluorine atom in its structure for labeling with fluorine-18. Thus, as a first step towards developing an ^{18}F-labeled third-generation radioligand, our laboratory synthesized six new fluorine-containing analogs of ER176—three isomers with a fluoro group and three with a trifluoromethyl group at each of three positions (*ortho*, *meta*, and *para*) of the pendant aryl ring (Fig. 1) (*10*). *In vitro* studies demonstrated that all six analogs had high affinity for human TSPO (K_i=1.2−7.0 nM) and could be successfully labeled with carbon-11 with good yield (66–81% decay-corrected) and excellent chemical (>95%) and radiochemical purities (>99%). Selecting the most promising radioligand among the six candidates to label with fluorine-18 would significantly reduce the time and cost of future investigations; however, *in vitro* data alone would not provide sufficient guidance for this decision.

The present study used *in vivo* performance in monkey brain to select the most promising of the six ^{11}C-labeled analog(s) of ER176 for subsequent ^{18}F-radiolabeling. The two primary performance criteria were BP_{ND} and the stability of V_T over time, which is an indirect measure of lack of radiometabolite accumulation in the brain. Both baseline and pre-blocked PET scans in monkey brain were obtained, and brain uptake was quantified as V_T using the radiometabolite-corrected arterial input function.

MATERIALS AND METHODS

Radiochemistry

^{11}C-ER176 was synthesized as previously described (*11*), with a molar activity of 106±65 GBq/µmol (*n*=4) at the time of injection and radiochemical purity of 97.1±4.4%.

Six fluorine-containing analogs of ER176 (Fig. 1) were labeled with carbon-11 at the tertiary amide group by ^{11}C-methylation of the respective *N*-desmethyl precursor as previously described (*10*). Briefly, the labeling precursors were synthesized by amidation of 4-oxo-3*H*-quinazoline-2-carboxylic acid followed by Pd-catalyzed coupling with appropriate fluorophenylboronic acids for the fluoro isomers—*o*-fluoro (SF12063), *m*-fluoro (SF12051), and *p*-fluoro (SF12052)—and trifluoromethylphenylboronic acids for the trifluoromethyl isomers—*o*-trifluoromethyl (SF12050), *m*-trifluoromethyl (SF12057), and *p*-trifluoromethyl (SF12054). Six ^{11}C-labeled TSPO radioligands were then obtained by methylation at the secondary amide group of the respective *N*-desmethyl precursors in dimethyl sulfoxide with ^{11}C-methyl iodide. The molar activity was 222±162 GBq/µmol (*n*=18) for the fluoro radioligands and 111±71 GBq/µmol (*n*=10) for the trifluoromethyl radioligands at the time of injection (Supplemental Table 1). The radiochemical purity of all radioligands was 99.6±0.5% (*n*=28).

Animals

In vivo experiments were performed in nine healthy male rhesus monkeys (body weight, 12.4±1.3 kg). Anesthesia was maintained with 1–2% isoflurane and 98% O_2 for the duration of the study. The head was firmly fixed by gauze and tapes to the camera bed holder. Body temperature was maintained with air blankets, and temperature, oxygen saturation, blood

pressure, and end-tidal CO_2 were monitored for the duration of the study. All animal studies were conducted in compliance with the Guide for the Care and Use of Laboratory Animals and were approved by the National Institute of Mental Health Animal Care and Use Committee.

PET Data Acquisition

The baseline PET scan was acquired for all radioligands (injected activity, 249±78 MBq) using a microPET Focus 220 scanner (Siemens Medical Solutions, Knoxville, TN, USA), with frame duration ranging from 30 seconds to 10 minutes. For the pre-blocked scans, racemic PK11195 (5 mg/kg) was intravenously administered 5-10 minutes before the radioligand. All PET scans were acquired for 120 minutes at baseline and 90 minutes after pre-blocking. Concurrent arterial blood sampling was performed in all scans to obtain a radiometabolite-corrected input function for quantification. PET images were reconstructed using Fourier rebinning algorithm plus two-dimensional filtered back projection with attenuation and scatter correction.

Measurement of Parent Radioactivity in Plasma

Fifteen blood samples were drawn from an implanted port in the femoral artery during the PET scan every 15 seconds for the first two minutes, followed by sampling at 3, 5, 10, 30, 60, 90, and 120 minutes (varying from 1.0 to 3.0 mL); 14 samples were drawn during the 90-minute PET scan. The parent radioligand was separated from radiometabolites, as previously described (*12*). Plasma parent and whole blood activity concentration were fitted with a triexponential function. The plasma free fraction (f_P) was measured by ultrafiltration, as previously described (*13*).

Kinetic Analysis

All kinetic analyses were performed using PMOD 3.9 (PMOD Technologies Ltd., Zurich, Switzerland). V_T was estimated with Logan graphical analysis (LGA) using 90 minutes of brain time-activity curves and the radiometabolite-corrected arterial input function for both baseline and pre-blocked studies. Details of the kinetic analysis are provided in the supplemental materials (*14*).

Estimating Ratio of Specific to Nondisplaceable Uptake

BP_{ND} was used to compare the performance of the six radioligands; this measure is a ratio of receptor-specific (V_S; V_T - V_{ND}) to nondisplaceable uptake (V_{ND}; free plus nonspecific binding) at equilibrium. In our opinion, BP_{ND} is a better binding measure than V_T because BP_{ND} directly quantifies specific binding. BP_{ND} is also more suitable than V_S because it is a "signal to noise" measurement that takes background into consideration. BP_{ND} was calculated as follows (*15*):

$$BP_{ND} = \frac{V_T - V_{ND}}{V_{ND}} = \frac{V_T}{V_{ND}} - 1$$

where V_T refers to V_T at baseline, and V_{ND} was estimated by the Lassen plot.

Because only unbound parent radioligand contributes to specific binding to the receptor, and because f_P was significantly different before and after pre-blocking (see Results), brain uptake and BP_{ND} were calculated and compared for the six radioligands using V_T and V_{ND} values corrected for f_P as V_T/f_P and V_{ND}/f_P, respectively.

Time Stability Analysis of V_T

To determine the minimal scan duration needed to reliably measure V_T and to indirectly assess whether radiometabolites enter the brain, time stability was evaluated by using 120

minutes of baseline PET data with truncated acquisition duration from 30 to 120 minutes in 10-minute increments. The identifiability of V_T was also evaluated as %SE at each truncated scan duration.

Ex Vivo Blood Cell Analysis

The utility of radioligand uptake was investigated in blood cells as a surrogate for brain uptake. Radioactivity concentration in *ex vivo* blood cells (C_{BC}) was calculated at both baseline and in pre-blocked studies as follows (*16*):

$$C_{BC} = C_{PL} + \frac{(C_{WB} - C_{PL})}{Hct}$$

Here, C_{BC}, C_{PL}, and C_{WB} indicate radioactivity concentrations in the blood cells, plasma, and whole blood, respectively, and *Hct* indicates hematocrit. The distribution volume in blood cells (V_{BC}) was then obtained by dividing C_{BC} by the radioactivity concentration of the parent radioligand in plasma and then corrected for f_P (V_{BC}/f_P). The correlation between V_{BC}/f_P and whole-brain V_T/f_P and between percentage blockade calculated using V_{BC}/f_P and whole-brain V_T/f_P were assessed using linear regression analysis.

Replication Study and Statistical Analysis

Based on the results of the first scans, replication studies were conducted for selected radioligands in different monkeys to confirm either the radioligands' most favorable properties or aberrant data. When multiple experiments were performed with the same radioligand, quantitative results are presented as mean ± standard deviation. Statistical significance was set at $P<0.05$. All statistical analyses were conducted with Prism 5 (GraphPad Software, La Jolla, CA, USA).

RESULTS

Uptake in Monkey Brain

Brain radioactivity at baseline increased rapidly and reached its peak SUV (2.7) at ~25 minutes post-injection (Figs. 2A, 2B) except for the *p*-trifluoromethyl radioligand, which showed very slow uptake with a time-to-peak of 75 minutes. The *m*-trifluoromethyl radioligand showed the highest peak uptake (SUV=3.4), and the *m*-fluoro radioligand showed the lowest peak uptake (2.6). The brain region with the highest peak SUV was the striatum (3.9), followed by the thalamus (3.2) and cerebellum (3.1); the parietal cortex had the lowest SUV (2.4). Peak radioactivity uptake in all regions was followed by a smooth decrease in radioactivity level; for example, radioactivity in the whole brain decreased by 37% at 90 minutes post-injection. In pre-blocked scans, all six radioligands showed a similar brain uptake pattern. Brain radioactivity rapidly increased and reached a peak SUV of 4.1 at 3.5 minutes post-injection, followed by a rapid decline and then a slow washout (Figs. 2C, 2D).

Plasma Concentration of Parent Radioligand

The concentration of parent radioligands in plasma peaked at 1.0–1.3 minutes after injection at baseline and then rapidly declined, followed by a slow terminal clearance phase. The fitting of plasma parent curves converged by tri-exponential function in all experiments (Fig. 3). The plasma parent fraction at baseline, expressed as a percentage of total plasma radioactivity, declined rapidly, and reached 50% at 25.6±11.6 minutes for the *m*-fluoro, *p*-fluoro, and *o*-trifluoromethyl radioligands (Supplemental Fig. 1). In contrast, the *o*-fluoro and the *m*-trifluoromethyl radioligand showed a slower decline, reaching 50% at 50.7±14.5 minutes after injection, and the *p*-trifluoromethyl radioligand exhibited unusually high plasma parent fraction

(>90%) during the entire 120 minutes of the scan. In pre-blocked scans, the parent radioactivity concentrations in plasma showed a rapid increase, reaching the peak at 1.0–1.5 minutes, followed by a fast washout and then a slow terminal clearance phase in all radioligands. As in our prior studies (*11*,*17*), the peak concentration of parent radioligand in plasma was much higher in the pre-blocked scans than in the baseline scans, because PK11195 blocks the distribution of radioligand to peripheral organs—like lung and kidneys—that have high densities of TSPO. The temporal changes of parent fraction in plasma were similar in all radioligands, characterized by a rapid decline that reached <50% by 30 minutes, with a subsequent gradual decline.

Reversed-phase high-performance liquid chromatography of plasma revealed at least five radiometabolites, all of which appeared less lipophilic than the parent radioligand. A lipophilic radiometabolite appeared in plasma from all radioligand experiments, except the baseline study of the *p*-trifluoromethyl radioligand. Nonetheless, the amount was negligible (0.07±0.08% of total plasma radioactivity across all arterial samples). The f_P was 17.3±8.2% at baseline for the fluoro radioligands, whereas it was significantly higher (22.3±11.3%) after pre-blocking (n=9, p=0.017). In contrast, there was no significant difference in f_P at baseline and after pre-blocking for the trifluoromethyl radioligands; f_P was 10.1±2.9% at baseline and 10.6±3.1% at pre-block (n=5, p=0.423).

Kinetic Analysis

Brain uptake was well quantified by LGA, which does not require specific compartment configurations. Regional brain uptake was reliably quantified as V_T with excellent identifiability (%SE<10%) in all baseline and pre-blocked studies. The trifluoromethyl radioligands generally

showed higher V_T/f_P (mL·cm^{-3}) for baseline and pre-blocked conditions than the fluoro radioligands (363 vs. 138 at baseline and 50 vs. 23 at pre-block, respectively) (Fig. 4). The *p*-trifluoromethyl radioligand had the highest V_T/f_P (493) at baseline, followed by the *m*-trifluoromethyl (411) and *o*-fluoro (223) radioligands (Table 1). The three brain regions with the highest V_T/f_P were the striatum (286), thalamus (283), and frontal cortex (269). The three with the lowest V_T/f_P were the cerebellum (208), amygdala (228), and occipital cortex (243). The percentage blockade by PK11195 was 82.5±7.3% and was similar for all six radioligands.

Estimating Ratio of Specific to Nondisplaceable Uptake

The *o*-fluoro radioligand exhibited the highest ratio of specific to nondisplaceable uptake (BP_{ND}, 12.1), followed by the *m*-trifluoromethyl (11.7) and *m*-fluoro (8.1) radioligands (Table 1). The Lassen plot analysis displayed excellent linear correlations (R^2>0.90) at high receptor occupancies (>87%) in all radioligands (Supplemental Fig. 2). Estimated V_{ND}/f_P (mL·cm^{-3}) values mainly ranged between 5.0 and 35.0, except for the *p*-trifluoromethyl radioligand (63.6). V_{ND}/f_P was smallest for the *p*-fluoro radioligands (7.9), followed by *m*-fluoro (9.8) and *o*-fluoro (16.6) radioligands (Table 1). As shown in Supplemental Table 2, the results were similar to the analysis without f_P correction.

Time Stability of V_T

The whole-brain V_T values asymptotically reached terminal values and converged within 10% of their terminal values by 70 minutes of a 120-minute scan (Figs. 5A, 5B). V_T values remained almost stable for the last 50 minutes, showing an average change of 4.7%, and could be quantified with excellent identifiability (%SE<5%) (Supplemental Fig. 3). The fluoro and

trifluoromethyl radioligands took a similar amount of time to achieve stable V_T values (70 minutes). The relatively stable V_T measurement over the 70–120-minute scan period suggested no significant accumulation of radiometabolites in the brain.

Performance Comparison with ^{11}C-ER176

o-Fluoro, *m*-trifluoromethyl, and *m*-fluoro radioligands showed similar or higher BP_{ND} than ^{11}C-ER176 (8.9), while the other three showed slightly lower values (Table 1). Regarding the time stability of V_T, it took a similar amount of time for whole-brain V_T of ^{11}C-ER176 and its six fluorine-containing analogs to reach and remain stable within 10% of their terminal values (90 vs. 70 minutes) (Fig. 5, Supplemental Fig. 4).

Correlation between Radioligand Uptake in the Blood Cells and Brain

Ex vivo blood cell uptake (V_{BC}/f_P) was well correlated with *in vivo* whole-brain V_T/f_P in both baseline (R^2=0.938, p<0.001) and pre-blocked (R^2=0.750, p=0.012) studies (Supplemental Fig. 5). The percent blockade of V_{BC}/f_P by PK11195 was also significantly correlated with that of whole-brain V_T/f_P (R^2=0.583, p=0.046).

DISCUSSION

Of the six ^{11}C-ER176 analogs developed by our laboratory, the present study found that the *o*-fluoro, *m*-trifluoromethyl, and *m*-fluoro compounds were the three most promising. All three had high BP_{ND} (the ratio of specific to nondisplaceable uptake) and stable V_T measured over time in monkey brain, consistent with the lack of radiometabolite accumulation.

Specifically, the *o*-fluoro radioligand had the third-highest V_T/f_P at baseline (120 mL·cm^{-3}), 96% of which was specifically bound to TSPO, and the highest BP_{ND} (12.1), making it potentially the most promising of all six ^{11}C-ER176 analogs. The *m*-trifluoromethyl radioligand showed the second-highest V_T/f_P at baseline (411 mL·cm^{-3}), high specific binding to TSPO (96%), and high BP_{ND} (11.7). The *m*-fluoro radioligand also showed high V_T/f_P at baseline (92 mL·cm^{-3}), high specific binding to TSPO (95.6%), and high BP_{ND} (8.1). For these three radioligands, V_T values reached 90% of terminal 120-minute values by 70 minutes and remained relatively stable thereafter with excellent identifiability (%SE<5%), suggesting that no significant radiometabolites accumulated in the brain.

In the present study, LGA was used to quantify and compare brain uptake across all six radioligands because neither the one- nor the two-tissue compartment models fitted perfectly for all studies. With LGA, V_T was quantified with excellent identifiability (%SE<10%) in all baseline and pre-blocked studies. Logan-derived V_{ND}/f_P and BP_{ND} values were within acceptable ranges and became less variable within each of the fluoro and trifluoromethyl radioligands. However, LGA tends to underestimate V_T and BP_{ND}, typically 10–20% depending on both the noise level and radioligand concentration (*18,19*). It should be noted that the degree of underestimation in this study remains uncertain; however, given the same target (TSPO) and similar performance measures, we believe that the underestimation, if any, would have been consistent across all six radioligands and led to the same finding—that is, that the *o*-fluoro, *m*-trifluoromethyl, and *m*-fluoro analogs were the three best candidates.

Evaluation of V_T stability with respect to scan duration allows one to: 1) determine the minimum scan time required to obtain a stable V_T and 2) indirectly check the possibility of radiometabolite(s) accumulating in the brain. Acceptable scan durations typically occur when V_T

in all regions approach 10% of a terminal value. If brain-penetrant radiometabolite(s) accumulate in the brain, V_T is expected to increase continuously, making the values unlikely to reach a plateau and stabilize. Whether radiometabolites enter and accumulate in the brain is critical for imaging human TSPO, especially in LABs who have low specific binding. Although some small differences were noted between the radioligands, the present study found that, for all six radioligands, whole-brain V_T at baseline reached 10% of terminal value by 70 minutes and 5% by 90 minutes. This similarity in time stability suggests that it is unlikely that radiometabolites interfered with brain uptake.

Interestingly, the present study found that *ex vivo* blood cells were a useful surrogate of brain tissue. Both V_{BC}—the distribution volume of the blood cells—at baseline and under pre-blocked conditions and the percentage blockade by PK11195 were well correlated with those of whole-brain V_T/f_P. The similarity between the two organs can be used to evaluate the radioligands that specifically bind to receptors expressed in both the brain and blood cells. For example, the blood cell analysis could be used as a quick screening tool for candidate radioligands or a non-imaging supplement to validate imaging results, thus aiding the development of new PET radioligands. However, the utility of *ex vivo* blood cells should be verified for individual radioligands because the two organs differ in their efflux systems and compartmental configurations.

One of the advantages of ^{11}C-ER176 is that it has adequately high TSPO-specific binding for quantification across all *rs6971* genotypes. A previous postmortem analysis of human brain tissue measured the *in vitro* binding affinities (K_i) to all *rs6971* genotypes for ER176 and these six fluorine-containing analogs (*8,10*). As summarized in Table 1, the *p*-trifluoromethyl compound showed the smallest ratio of 0.8 (i.e., binding affinity difference) between high-

affinity binders and LABs, followed by ER176 (1.3), the *m*-trifluoromethyl (2.0) compound, the three fluoro compounds (2.7–2.9), and the *o*-trifluoromethyl (5.4) compound. Building on this finding, all six analogs investigated here are expected to achieve adequately high specific signal in LABs, at least higher than PBR28 (55.0) *(5)*, which has been the most widely used of the second-generation TSPO radioligands.

Taken together, these *in vitro* and *in vivo* data suggest that the *o*-fluoro, *m*-trifluoromethyl, and *m*-fluoro compounds appear to be the most promising analogs. However, all six radioligands performed well and with only small inter-ligand differences (Table 1). For example, the three fluoro radioligands exhibited similar BP_{ND} (4.8–12.1), time stability of V_T (all achieved stable V_T by 70 minutes), and binding affinity ratios (2.7–2.9), and all of these measures were comparable to those of ^{11}C-ER176. Nevertheless, unexpected labeling issues (e.g., unsatisfactory yield, or perhaps only marginally acceptable molar activity for labeling trifluoromethyl groups) for fluorine-18 radioligands may also arise in their development, limiting the use of particular radioligands despite solid performances in their ^{11}C-labeled forms. Thus, though the candidate radioligands have now been ranked, priorities for subsequent ^{18}F-radiolabeling will also be affected by the time and effort needed for radiochemistry. Moving forward, none of the six compounds will be excluded.

The underlying assumption of this study is that ^{18}F-labeled radioligands will perform similarly to their ^{11}C -labeled versions. However, the performance of an ^{11}C-labeled radioligand does not always guarantee success in its ^{18}F-labeled form. ^{18}F-labeling at a position different from an ^{11}C position in the molecular structure may change the spectrum of radiometabolites and generate unexpected brain-penetrating radiometabolites. Defluorination may also occur to confound the accurate quantification of receptor-specific brain uptake. Although strategic

positioning of an ^{18}F label can reduce the production of these troublesome radiometabolites, the *in vivo* metabolism of a radioligand (e.g., the sites of metabolic cleavage) is not always predictable and further varies across species (*20*).

CONCLUSION

The six fluorine-containing analogs of ER176 were relatively easily labeled with carbon-11. PET imaging in monkey brain showed that all six ^{11}C-labeled analogs had good BP_{ND} and good time stability of V_T. Of the six ligands, the *o*-fluoro, *m*-trifluoromethyl, and *m*-fluoro compounds were arguably the three best candidates to radiolabel with fluorine-18, a process that is expected to be quite challenging.

DISCLOSURE

This study was funded by the Intramural Research Program of the National Institute of Mental Health, National Institutes of Health (ZIAMH002795 and ZIAMH002793). The authors have no conflict of interest to disclose, financial or otherwise

ACKNOWLEDGMENTS

The authors thank the dedicated staff of the Molecular Imaging Branch of the NIMH, the PET Department of the NIH Clinical Center, and the NIMH veterinary staff for help in completing the studies.

KEY POINTS

Question: Which are the most promising fluorine-containing analogs of ^{11}C-ER176 for subsequent ^{18}F-radiolabeling?

Pertinent Findings: This study used generic carbon-11 labeling and *in vivo* performance in monkey brain—BP_{ND} and time stability of V_T—to select the most promising analogs among six candidates. The *o*-fluoro, *m*-trifluoromethyl, and *m*-fluoro compounds were arguably the three best candidates because they showed the three highest BP_{ND} values as well as good time stability of V_T.

Implications for Patient Care: The development of an ^{18}F-labeled radioligand based on ^{11}C-ER176 would allow greater flexibility and more widespread use of TSPO PET.

REFERENCES

1. Papadopoulos V, Baraldi M, Guilarte TR, et al. Translocator protein (18kDa): new nomenclature for the peripheral-type benzodiazepine receptor based on its structure and molecular function. *Trends Pharmacol Sci.* 2006;27:402-409.

2. Meyer JH, Cervenka S, Kim MJ, Kreisl WC, Henter ID, Innis RB. Neuroinflammation in psychiatric disorders: PET imaging and promising new targets. *Lancet Psychiatry.* 2020;7:1064-1074.

3. Chauveau F, Boutin H, Van Camp N, Dolle F, Tavitian B. Nuclear imaging of neuroinflammation: a comprehensive review of [^{11}C]PK11195 challengers. *Eur J Nucl Med Mol Imaging.* 2008;35:2304-2319.

4. Le Fur G, Perrier ML, Vaucher N, et al. Peripheral benzodiazepine binding sites: effect of PK 11195, 1-(2-chlorophenyl)-N-methyl-N-(1-methylpropyl)-3-isoquinolinecarboxamide. I. In vitro studies. *Life Sci.* 1983;32:1839-1847.

5. Kreisl WC, Jenko KJ, Hines CS, et al. A genetic polymorphism for translocator protein 18 kDa affects both in vitro and in vivo radioligand binding in human brain to this putative biomarker of neuroinflammation. *J Cereb Blood Flow Metab.* 2013;33:53-58.

6. Owen DR, Yeo AJ, Gunn RN, et al. An 18-kDa translocator protein (TSPO) polymorphism explains differences in binding affinity of the PET radioligand PBR28. *J Cereb Blood Flow Metab.* 2012;32:1-5.

7. Kreisl WC, Kim MJ, Coughlin JM, Henter ID, Owen DR, Innis RB. PET imaging of neuroinflammation in neurological disorders. *Lancet Neurol.* 2020;19:940-950.

8. Ikawa M, Lohith TG, Shrestha S, et al. 11C-ER176, a Radioligand for 18-kDa Translocator Protein, Has Adequate Sensitivity to Robustly Image All Three Affinity Genotypes in Human Brain. *J Nucl Med.* 2017;58:320-325.

9. Fujita M, Kobayashi M, Ikawa M, et al. Comparison of four ^{11}C-labeled PET ligands to quantify translocator protein 18 kDa (TSPO) in human brain: (R)-PK11195, PBR28, DPA-713, and ER176-based on recent publications that measured specific-to-non-displaceable ratios. *EJNMMI Res.* 2017;7:84.

10. Siméon FG, Lee JH, Morse CL, et al. Synthesis and screening in mice of fluorine-containing PET radioligands for TSPO: discovery of a promising ^{18}F-labeled ligand. *J Med Chem.* https://doi.org/10.1021/acs.jmedchem.1c01562.

11. Zanotti-Fregonara P, Zhang Y, Jenko KJ, et al. Synthesis and evaluation of translocator 18 kDa protein (TSPO) positron emission tomography (PET) radioligands with low binding sensitivity to human single nucleotide polymorphism rs6971. *ACS Chem Neurosci.* 2014;5:963-971.

12. Zoghbi SS, Shetty HU, Ichise M, et al. PET imaging of the dopamine transporter with ^{18}F-FECNT: a polar radiometabolite confounds brain radioligand measurements. *J Nucl Med.* 2006;47:520-527.

13. Gandelman MS, Baldwin RM, Zoghbi SS, Zea-Ponce Y, Innis RB. Evaluation of ultrafiltration for the free-fraction determination of single photon emission computed tomography (SPECT) radiotracers: beta-CIT, IBF, and iomazenil. *J Pharm Sci.* 1994;83:1014-1019.

14. Yasuno F, Brown AK, Zoghbi SS, et al. The PET radioligand [^{11}C]MePPEP binds reversibly and with high specific signal to cannabinoid CB1 receptors in nonhuman primate brain. *Neuropsychopharmacology.* 2008;33:259-269.

15. Innis RB, Cunningham VJ, Delforge J, et al. Consensus nomenclature for in vivo imaging of reversibly binding radioligands. *J Cereb Blood Flow Metab.* 2007;27:1533-1539.

16. Kanegawa N, Collste K, Forsberg A, et al. In vivo evidence of a functional association between immune cells in blood and brain in healthy human subjects. *Brain Behav and Immun.* 2016;54:149-157.

17. Briard E, Zoghbi SS, Imaizumi M, et al. Synthesis and evaluation in monkey of two sensitive 11C-labeled aryloxyanilide ligands for imaging brain peripheral benzodiazepine receptors in vivo. *J Med Chem.* 2008;51:17-30.

18. Logan J, Fowler JS, Volkow ND, Ding YS, Wang GJ, Alexoff DL. A strategy for removing the bias in the graphical analysis method. *J Cereb Blood Flow Metab.* 2001;21:307-320.

19. Slifstein M, Laruelle M. Effects of statistical noise on graphic analysis of PET neuroreceptor studies. *J Nucl Med.* 2000;41:2083-2088.

20. Pike VW. PET radiotracers: crossing the blood-brain barrier and surviving metabolism. *Trends Pharmacol Sci.* 2009;30:431-440.

FIGURE LEGENDS

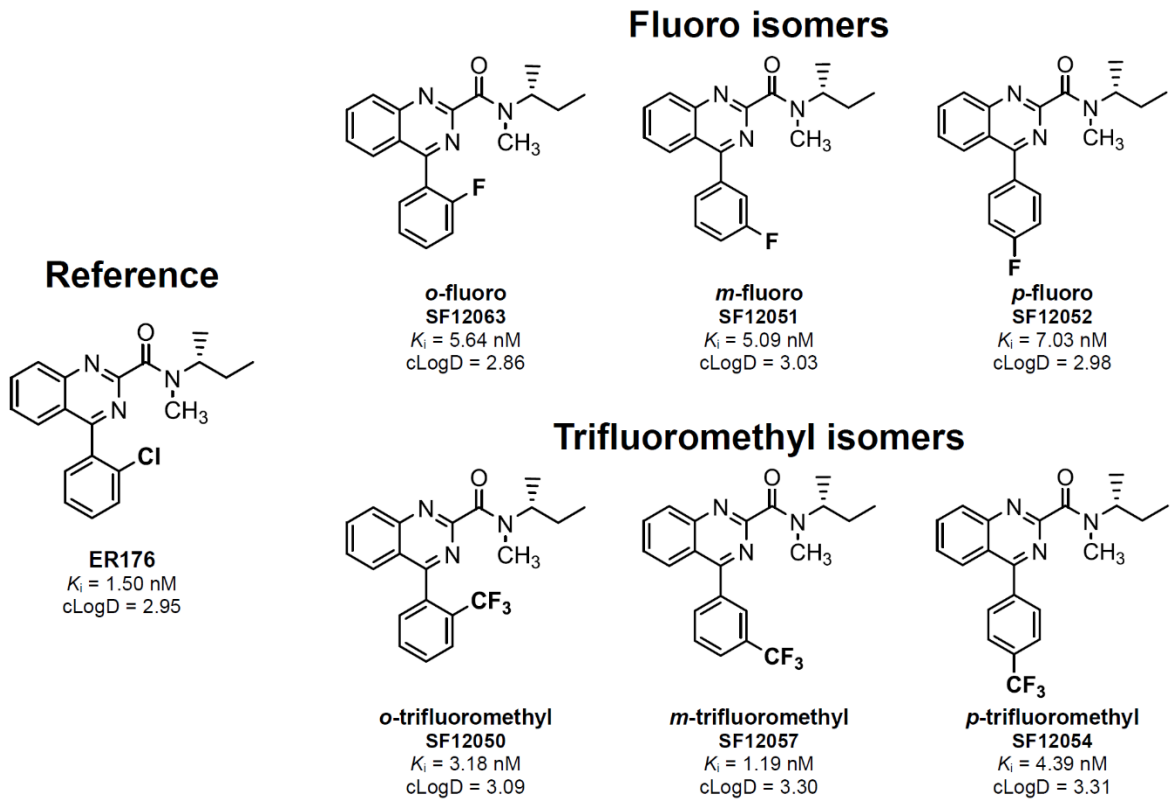

Figure 1. Chemical structures of ^{11}C-ER176 and six fluorine-containing analogs.

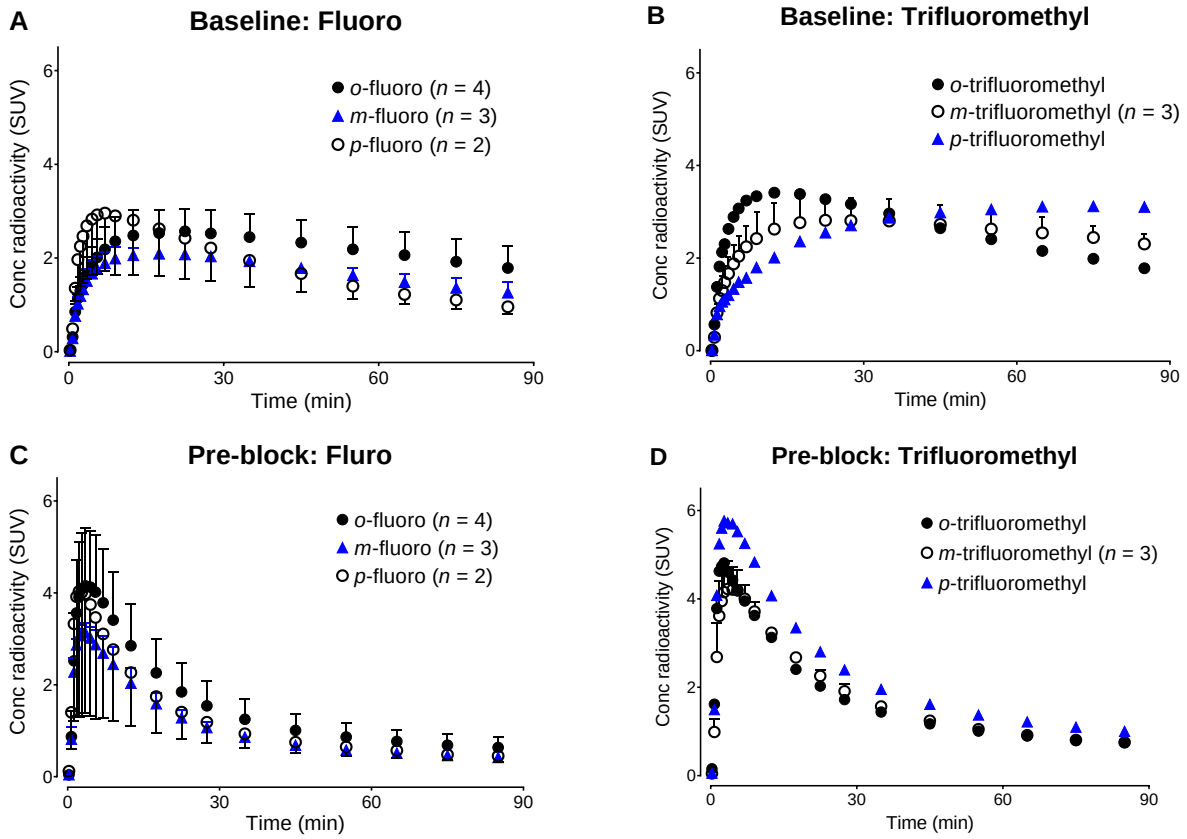

Figure 2. Time-activity curves of whole-brain uptake in baseline and pre-blocked scans for the fluoro (A, C) and trifluoromethyl (B, D) radioligands. Point and bar represent mean standardized uptake value (SUV) and standard deviation, respectively.

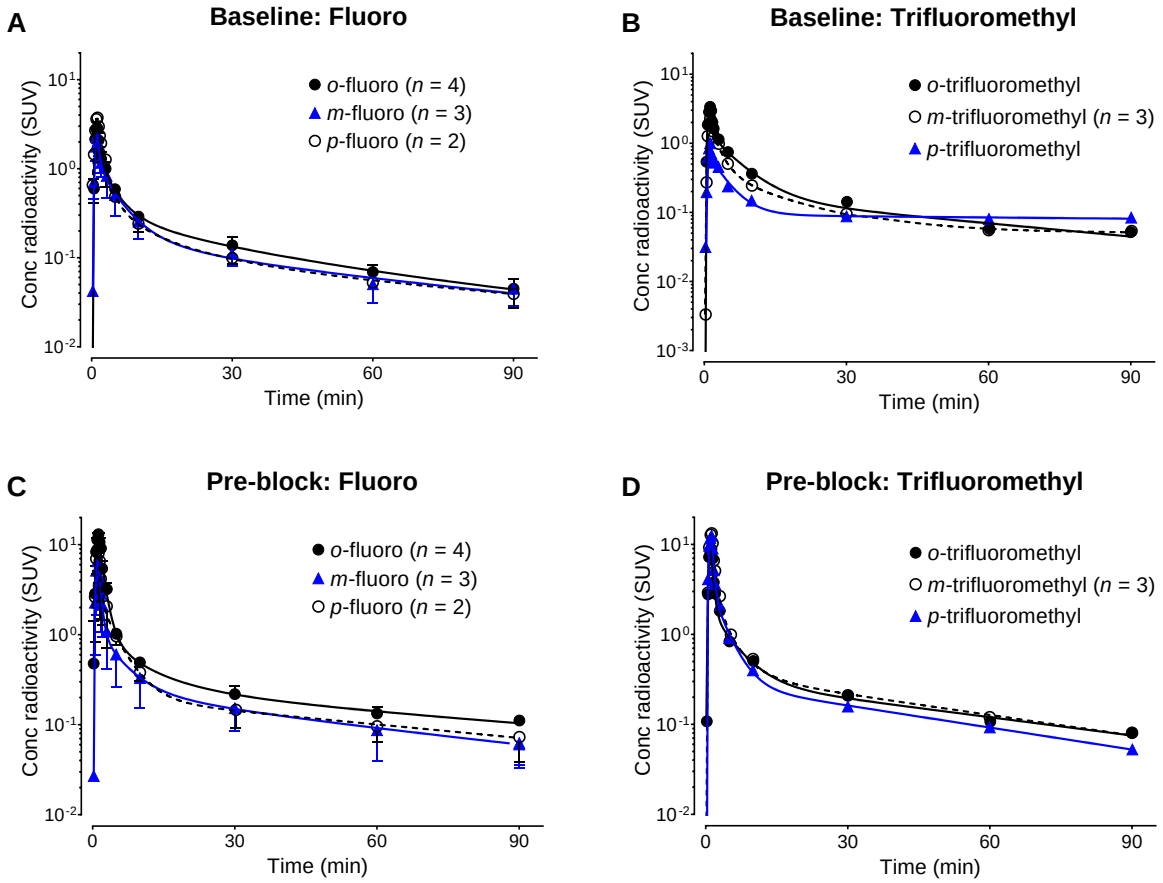

Figure 3. Time course of radioactivity concentrations in plasma at baseline and in pre-blocked scans for the fluoro (A, C) and trifluoromethyl (B, D) radioligands. Point and bar represent mean standardized uptake value (SUV) and standard deviation, respectively.

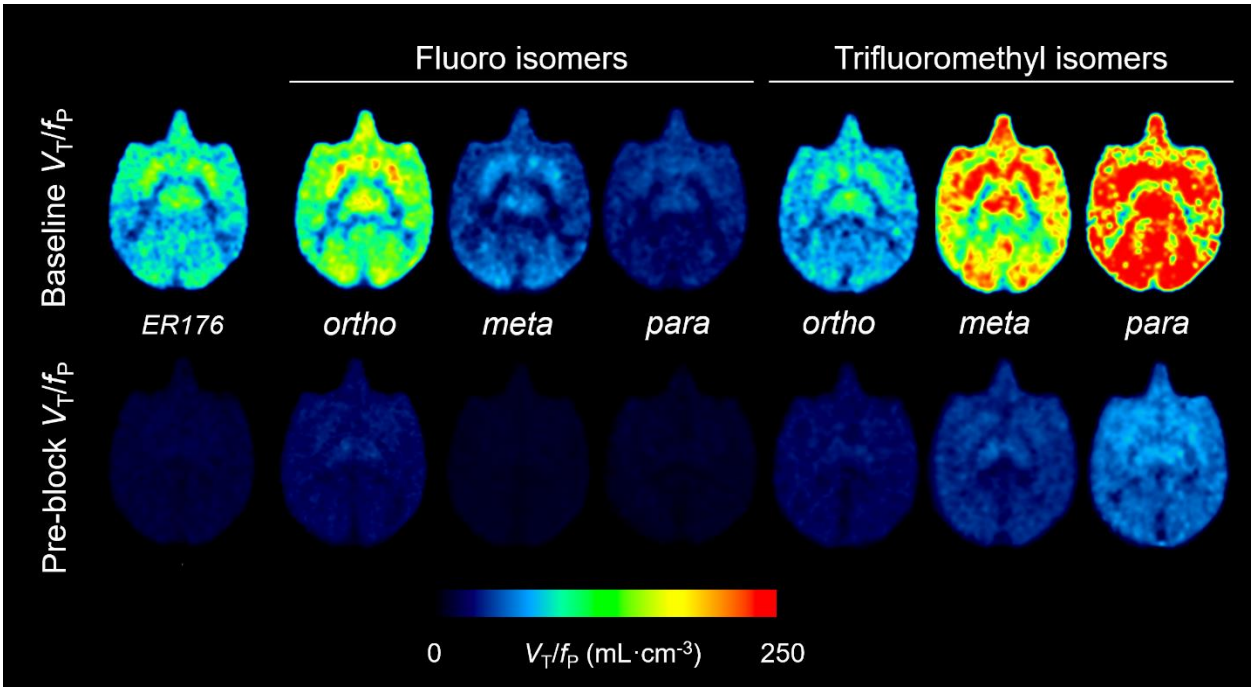

Figure 4. Average parametric images of total TSPO binding (V_T/f_P) for ^{11}C-ER176 and six analogs in monkey brain at baseline (top row) and pre-blocked scans (bottom row). Each V_T/f_P image was generated using 0–90 minutes of PET data obtained via Logan graphical analysis.

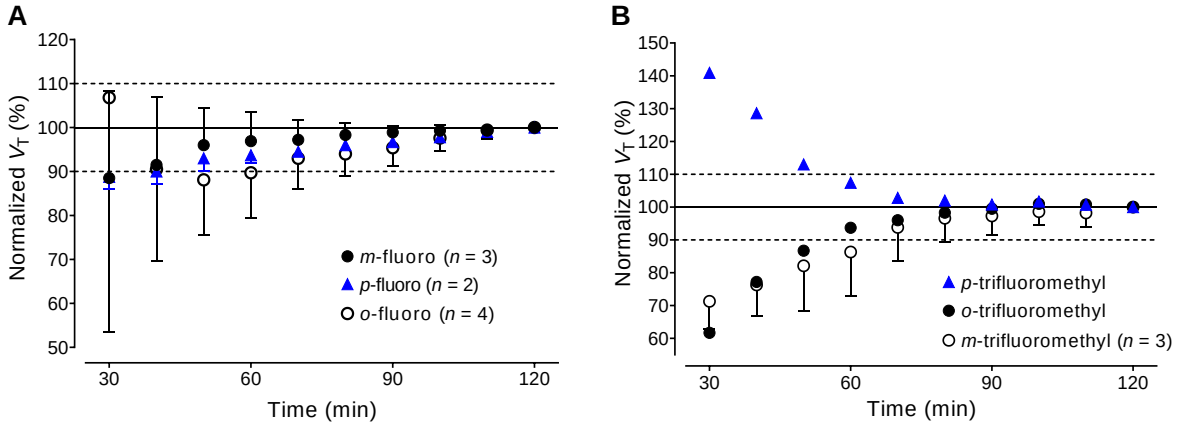

Figure 5. Time stability analysis of whole-brain total distribution volume (V_T) for the fluoro (A) and trifluoromethyl (B) radioligands. V_T was calculated via Logan graphical analysis and normalized to the terminal V_T value at 120 minutes. Points represent the mean normalized V_T (±SD).

Table 1. Comparison of total distribution volume (V_T/f_P), occupancy, nondisplaceable distribution volume (V_{ND}/f_P), and nondisplaceable binding potential (BP_{ND}) of the whole brain among ^{11}C-ER176 and six fluorine-containing analogs.

	V_T/f_P (mL·cm^{-3})						
	Baseline	Pre-block	Blockade (%)	Occupancy (%)	V_{ND}/f_P (mL·cm^{-3})	BP_{ND}	Binding affinity ratio[a]
Reference							
^{11}C-ER176	185.8	21.3	88.5	98.6	18.6	8.9	1.3
Fluoro							
o-fluoro	223.8	33.3	85.0	92.9	16.6	12.1	2.8
m-fluoro	92.2	12.7	84.9	95.6	9.8	8.1	2.7
p-fluoro	45.3	13.4	70.3	89.0	7.9	4.8	2.9
Trifluoromethyl							
o-trifluoromethyl	119.7	31.5	73.5	87.1	18.5	5.5	5.5
m-trifluoromethyl	411.0	47.6	86.9	95.0	32.6	11.7	2.0
p-trifluoromethyl	493.0	73.6	84.8	97.7	63.6	6.7	0.8

Data are presented as mean.

[a]Ratio of binding affinity (K_i in nM) in low-affinity binders to that of high-affinity binders.

GRAPHICAL ABSTRACT

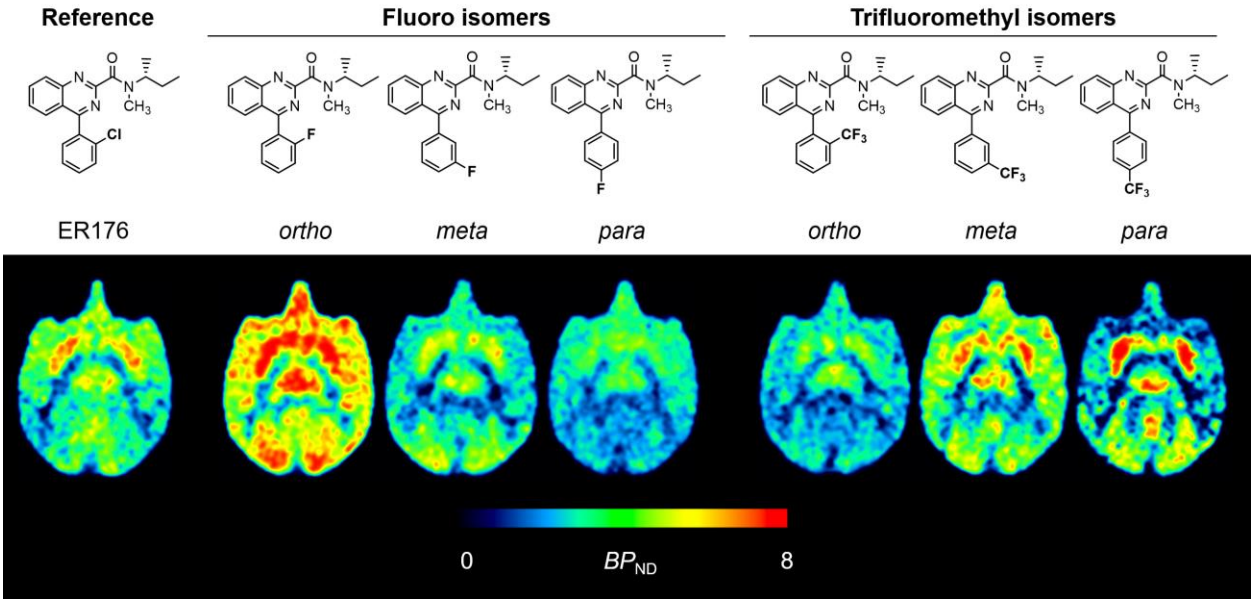

SUPPLEMENT

Kinetic Analysis

All kinetic analyses were performed using PMOD 3.9 (PMOD Technologies Ltd., Zurich, Switzerland). PET images were coregistered to a standardized monkey magnetic resonance imaging template (*1*). Thirty-four predefined brain regions of interest from the template were applied to the coregistered PET image to obtain regional time-activity curves. Brain uptake was expressed as a standardized uptake value (SUV), which normalizes for injected radioactivity and body weight.

Distribution volume (V_T) was estimated for different regions. For a more robust estimation of V_T, Logan graphical analysis was used and applied to compare performance across all radioligands. For both baseline and pre-blocked conditions, only 90 minutes of brain time-activity curves and the radiometabolite-corrected arterial input function were used. Starting PET frames used for regression were selected based on the equilibration time (t^*) of the whole brain. The equilibration time was automatically determined for the maximum allowed regression error of 10%. The equilibration time was similar for the six radioligands and generally ranged between 10 and 20 minutes. The identifiability of V_T (i.e., percent standard error estimated from the theoretical parameter covariance matrix) was also determined. Parametric images of brain TSPO binding were generated for visual comparison of brain uptake among radioligands as well as between baseline and pre-blocked studies.

SUPPLEMENTAL REFERENCES

1. Yasuno F, Brown AK, Zoghbi SS, et al. The PET radioligand [11C]MePPEP binds reversibly and with high specific signal to cannabinoid CB1 receptors in nonhuman primate brain. *Neuropsychopharmacology.* 2008;33:259-269.

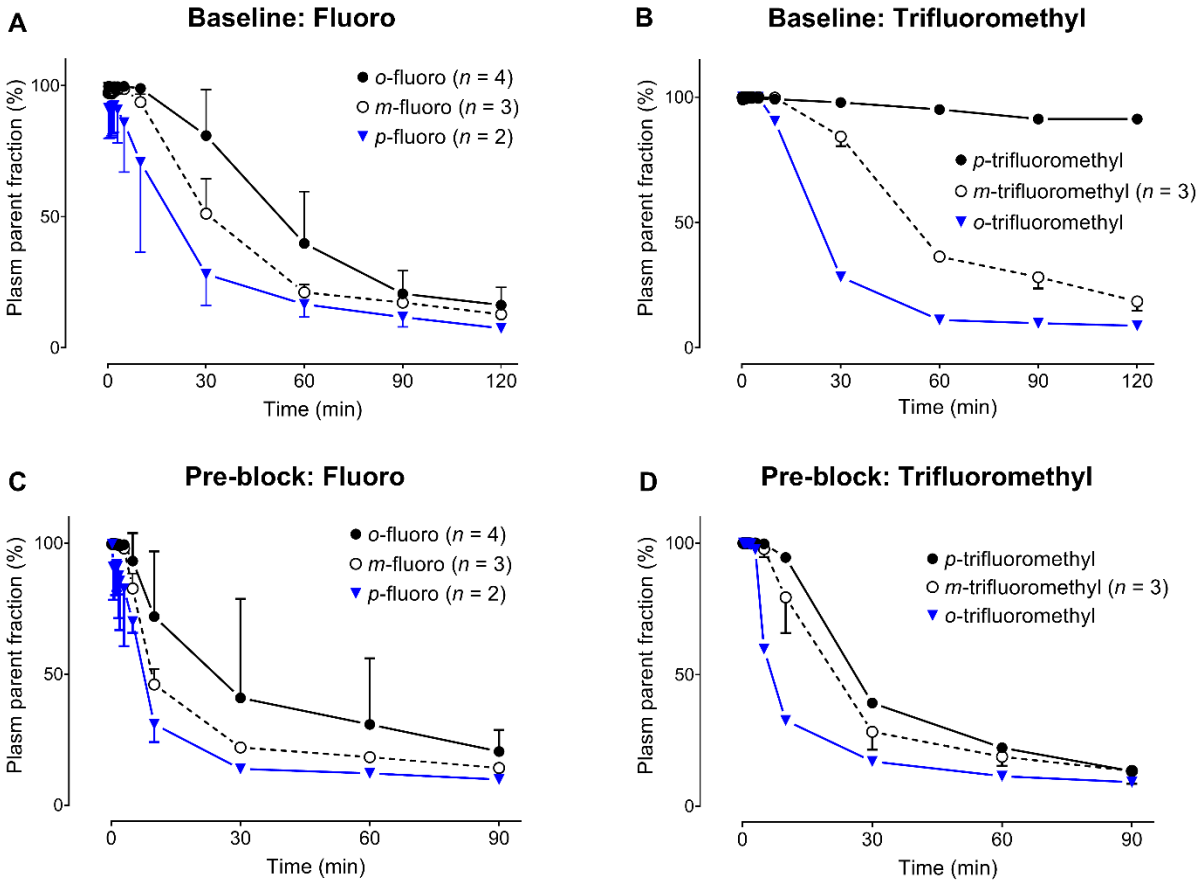

Supplemental Figure 1. Time course of parent fraction in plasma at baseline and for pre-blocked scans for the fluoro (A, C) and trifluoromethyl (B, D) radioligands.

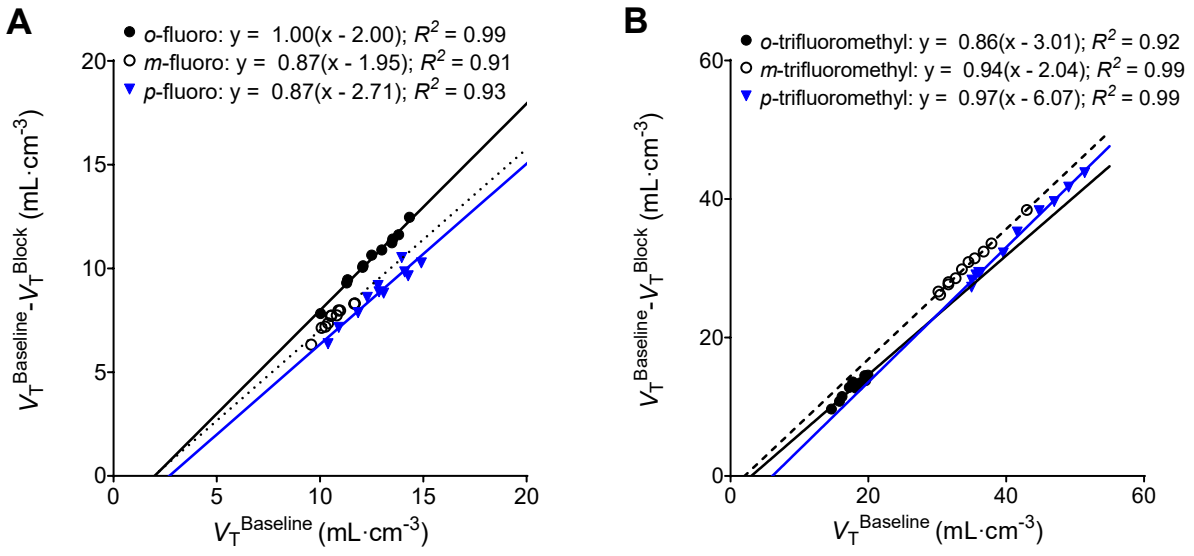

Supplemental Figure 2. Lassen plot to determine receptor occupancy and nondisplaceable distribution volume (V_{ND}/f_P) of the fluoro (A) and trifluoromethyl (B) radioligands in monkey brain. One representative data point is plotted for the radioligands with multiple replication studies.

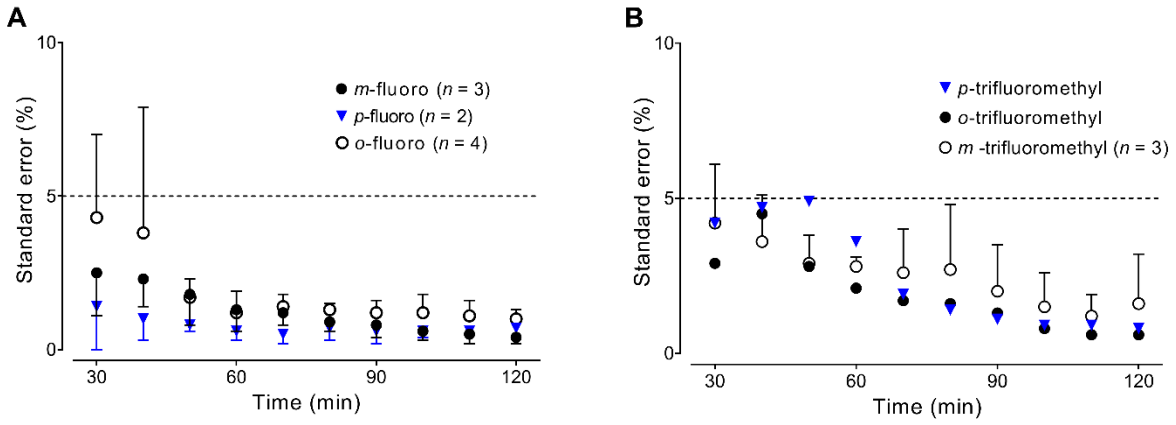

Supplemental Figure 3. Identifiability of whole-brain total distribution volume (V_T) for the fluoro (A) and trifluoromethyl (B) radioligands. V_T was calculated via Logan graphical analysis and normalized to the terminal V_T value at 120 minutes. Points represent the mean normalized V_T (± SD).

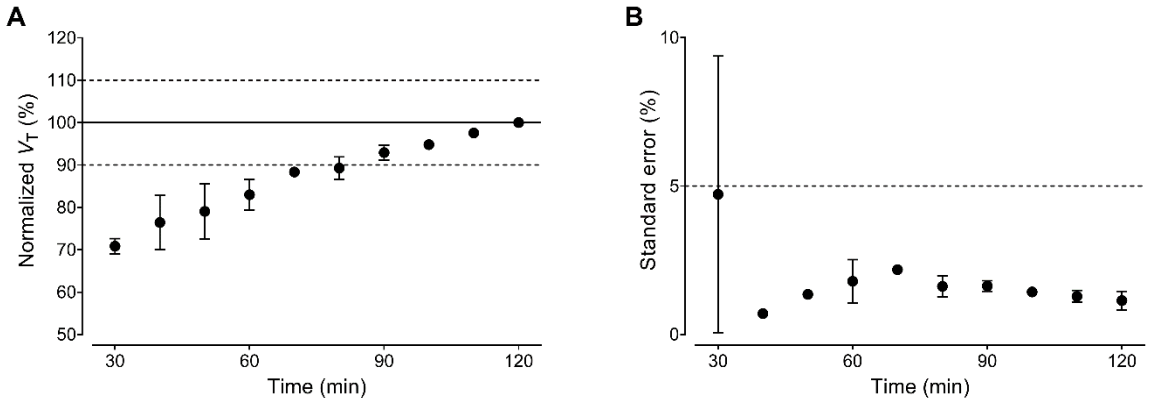

Supplemental Figure 4. Time-stability analysis (A) and identifiability (B) of whole-brain total distribution volume (V_T) for ^{11}C-ER176. V_T was calculated via Logan graphical analysis and normalized to the terminal V_T value at 120 minutes. Points represent the mean normalized V_T (± SD).

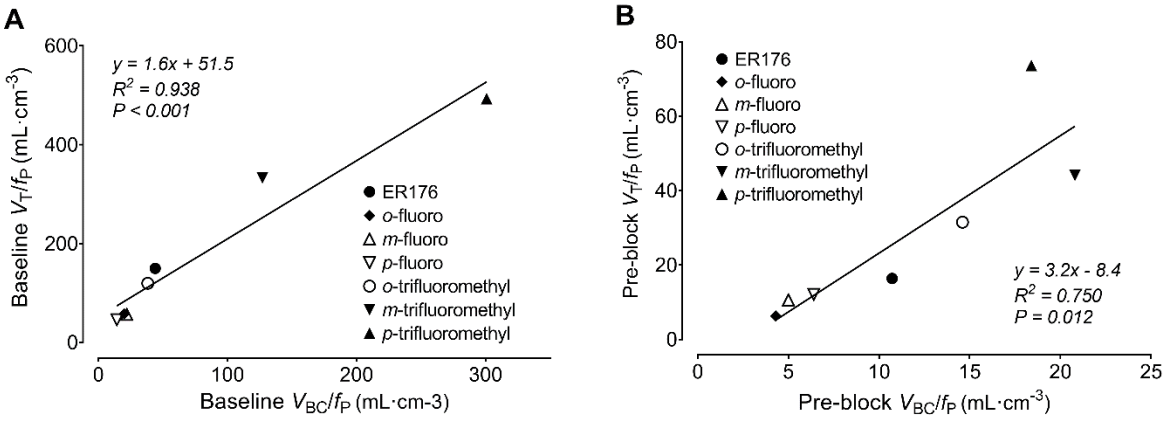

Supplemental Figure 5. The correlation between distribution volume in blood cells corrected for plasma free fraction (V_{BC}/f_P) and whole-brain distribution volume (V_T/f_P) for baseline (A) and pre-blocked (B) scans.

Supplemental Table 1. Summary of experimental protocols for six fluorine-containing analogs of ^{11}C-ER176

	Reference	Fluoro			Trifluoromethyl		
Radioligand	^{11}C-ER176	*o*-fluoro	*m*-fluoro	*p*-fluoro	*o*-trifluoromethyl	*m*-trifluoromethyl	*p*-trifluoromethyl
No. of studies	2	4	3	2	1	3	1
Weight (kg)	11.1	12.9	11.3	12.8	13.9	12.3	14.4
Injected activity (MBq)	246	241	300	274	272	242	269
Molar activity (MBq/nmol)	107	132	341	223	88	87	204
Injected mass (nmol/kg)	0.29	0.16	0.10	0.16	0.22	0.40	0.09

Data are presented as mean.

Supplemental Table 2. Comparison of total distribution volume (V_T), occupancy, nondisplaceable distribution volume (V_{ND}), and nondisplaceable binding potential (BP_{ND}) of the whole brain among ^{11}C-ER176 and six fluorine-containing analogs.

	V_T (mL·cm^{-3})						
	Baseline	Pre-block	Blockade (%)	Occupancy (%)	V_{ND} (mL·cm^{-3})	BP_{ND}	Binding affinity ratio[a]
Reference							
^{11}C-ER176	20.5	2.9	85.4	98.3	2.5	6.8	1.3
Fluoro							
o-fluoro	18.9	3.4	81.1	91.9	2.0	9.6	2.8
m-fluoro	17.9	3.3	78.1	90.0	2.6	5.9	2.7
p-fluoro	12.2	3.8	69.2	87.0	2.7	3.7	2.9
Trifluoromethyl							
o-trifluoromethyl	17.8	5.1	71.4	86.0	3.0	4.9	5.5
m-trifluoromethyl	35.7	4.3	87.1	95.3	2.9	11.6	2.0
p-trifluoromethyl	41.0	7.0	82.6	97.3	6.1	5.7	0.8

Data are presented as mean.

[a] Ratio of binding affinity (K_i in nM) in low-affinity binders to that of high-affinity binders.